

Bilayer-Mediated Clustering and Functional Interaction of MscL Channels

Stephan L. Grage,^{††} Asbed M. Keleshian,[§] Tamta Turdzeladze,^{‡¶} Andrew R. Battle,^{§||} Wee C. Tay,[§] Roland P. May,^{††} Stephen A. Holt,^{‡‡} Sonia Antoranz Contera,^{§§} Michael Haertlein,^{††} Martine Moulin,^{††} Prithwish Pal,^{§||} Paul R. Rohde,^{§||} V. Trevor Forsyth,^{††¶¶} Anthony Watts,^{|||} Kerwyn Casey Huang,^{†††*} Anne S. Ulrich,^{††¶*} and Boris Martinac^{§||†††*}

[†]Karlsruhe Institute of Technology, Institute of Biological Interfaces (IBG-2), Karlsruhe, Germany; [‡]DFG-Center for Functional Nanostructures, Karlsruhe, Germany; [§]School of Biomedical Sciences, University of Queensland, Brisbane, Australia; [¶]Karlsruhe Institute of Technology, Institute of Organic Chemistry, Karlsruhe, Germany; ^{||}Victor Chang Cardiac Research Institute, Darlinghurst, Australia; ^{††}Partnership for Structural Biology, Institut Laue-Langevin, Grenoble, France; ^{‡‡}ISIS, Rutherford Appleton Laboratory, Science and Technology Facilities Council, Didcot, United Kingdom; ^{§§}Department of Physics, University of Oxford, Oxford, United Kingdom; ^{¶¶}EPSAM/ISTM, Keele University, Staffordshire, United Kingdom; ^{|||}Biomembrane Structure Unit, Department of Biochemistry, Oxford, University of Oxford, United Kingdom; ^{†††}Department of Bioengineering, Stanford University, Stanford, California; and ^{†††*}St Vincent's Clinical School, University of New South Wales, Sydney, Australia

ABSTRACT Mechanosensitive channels allow bacteria to respond to osmotic stress by opening a nanometer-sized pore in the cellular membrane. Although the underlying mechanism has been thoroughly studied on the basis of individual channels, the behavior of channel ensembles has yet to be elucidated. This work reveals that mechanosensitive channels of large conductance (MscL) exhibit a tendency to spatially cluster, and demonstrates the functional relevance of clustering. We evaluated the spatial distribution of channels in a lipid bilayer using patch-clamp electrophysiology, fluorescence and atomic force microscopy, and neutron scattering and reflection techniques, coupled with mathematical modeling of the mechanics of a membrane crowded with proteins. The results indicate that MscL forms clusters under a wide range of conditions. MscL is closely packed within each cluster but is still active and mechanosensitive. However, the channel activity is modulated by the presence of neighboring proteins, indicating membrane-mediated protein-protein interactions. Collectively, these results suggest that MscL self-assembly into channel clusters plays an osmoregulatory functional role in the membrane.

INTRODUCTION

The mechanosensitive channel of large conductance (MscL) is a homopentameric protein that is gated by membrane tension. It primarily acts as an emergency relief valve to protect bacterial cells from lysis during periods of hypoosmotic shock (1). In its open conformation, the channel has a nonselective pore ~3 nm in diameter (2,3) that allows the rapid escape of cytoplasmic osmolytes.

Clustering of channels has been demonstrated in several systems, most notably acetylcholine receptors and glycine receptors, and in both cases the underlying mechanism was attributed to specialized proteins, such as gephyrin (4,5), that specifically anchor the receptors at predetermined locations. Lipid raft formation has been postulated as another mechanism that leads to membrane-protein clustering (e.g., for the sodium-potassium ATPase in cerebellar granular cells (6)). More recently, very weak homophilic protein-protein interactions were shown to lead to significant protein self-assembly within membranes, as observed for syntaxins (7). Clustering of membrane proteins due to membrane-mediated interactions has also been observed in ryanodine receptors (8,9), gramicidin A channels (10),

the bacterial potassium channel KcsA (11), and rhodopsin (12). Although there is increasing evidence that proteins in general assemble in clusters (13), clustering has not yet been demonstrated for the majority of membrane proteins, including MscL.

As is the case for most membrane proteins, the function of MscL has been regarded as a result of its architecture and response to the lipid environment (14,15). Most studies have focused on individual proteins and assumed no interactions with neighboring proteins. In the study presented here, we systematically obtained observations that are not in accordance with results obtained from isolated channels. Instead of independent and randomly distributed channels, we observed the formation of MscL clusters in all of the lipid systems examined, using a combination of structural techniques (small-angle neutron scattering (SANS), atomic force microscopy (AFM), and neutron reflection), fluorescence microscopy, and patch-clamp recording.

Even though clustering has been considered primarily as a biophysical property of MscL under in vitro conditions, the underlying principles of self-assembly may also play a role in the in vivo behavior of MscL. First, it has been reported that native expression levels of MscL increase from their low levels of approximately five copies per cell in various stages of cell growth (16). Second, fluorescence images from *Escherichia coli* expressing MscL-GFP fusion proteins suggest that the channel distribution is nonuniform during the early exponential phase of growth, and

Submitted July 23, 2010, and accepted for publication January 4, 2011.

*Correspondence: b.martinac@victorchang.edu.au or anne.ulrich@kit.edu or kchuang@stanford.edu

Dr. Stephen A. Holt's present address is Bragg Institute, ANSTO, Locked Bag 2001, Kirrawee DC, New South Wales, 2232 Australia.

Editor: Ka Yee C. Lee.

apparently has a higher density at the bacterial poles (16). The underlying mechanism of this nonuniformity is presently unclear, but the nonuniformity suggests that MscL channels may form clusters if they are segregated within their native environment. In this study, we used a combination of complementary techniques and liposome reconstitution methods to explore the clustering of MscL channels reconstituted over a wide range of protein/lipid ratios in lipid bilayers of varying lipid composition.

MATERIALS AND METHODS

Details about the MscL protein purification and reconstitution, fluorescence and AFM microscopy, patch-clamp recording, SANS and neutron reflection experiments, and theoretical modeling are described in the [Supporting Material](#).

RESULTS

Nonuniform distribution of MscL channels in liposome blisters

Results from simulation studies with uniformly distributed channels, assuming a channel area of 24 nm^2 (17,18) and a patch area of $1.6 \mu\text{m}^2$, indicate that for protein/lipid ratios ranging from 1:50 to 1:8000 (w/w), the distribution of the number of channels per patch should be binomial and can be approximated by a Poisson distribution. Confocal images of fluorescently labeled spheroplasts and of blisters (large unilamellar structures induced in multilamellar liposomes

by magnesium chloride (19), prepared by the dehydration/rehydration method) containing Alexa-488-labeled MscL at a protein/lipid ratio of 1:1000 (w/w) showed a distinct nonuniform distribution of fluorescence along the bilayer (Fig. 1, *a–c*). In contrast, images of the same blister containing 1% rhodamine-labeled DOPE revealed a uniform distribution of the lipid (Fig. 1, *b* and *c*). To confirm the nonuniformity of MscL distribution, we examined blisters from a similar preparation using the patch-clamp method. We determined the distribution of the number of channels by applying maximum suction (see [Materials and Methods](#)) and compared it with a Poisson distribution (an example of a patch with four channels is depicted in Fig. 1 *d*). The presence of subconductance levels (20) complicated accurate counting of the total number of concurrent openings when the number of channels was large. Therefore, all patches containing >30 channels were grouped together (Fig. 1 *e*). The cumulative distribution of the number of channels (data from 72 patches) differed significantly from the cumulative Poisson distribution.

A significant deviation from Poisson statistics was also evident when MscL was reconstituted with pure DOPC or with mixtures of DOPC and DOPE, using the sucrose method (21). The standard deviations of the distributions of the number of channels were much larger than expected for a uniform distribution, with trends similar to those observed for azolectin (Table S1). We noticed that the efficiency of insertion of MscL protein into the bilayer can sometimes depend on the particular lipids used; in

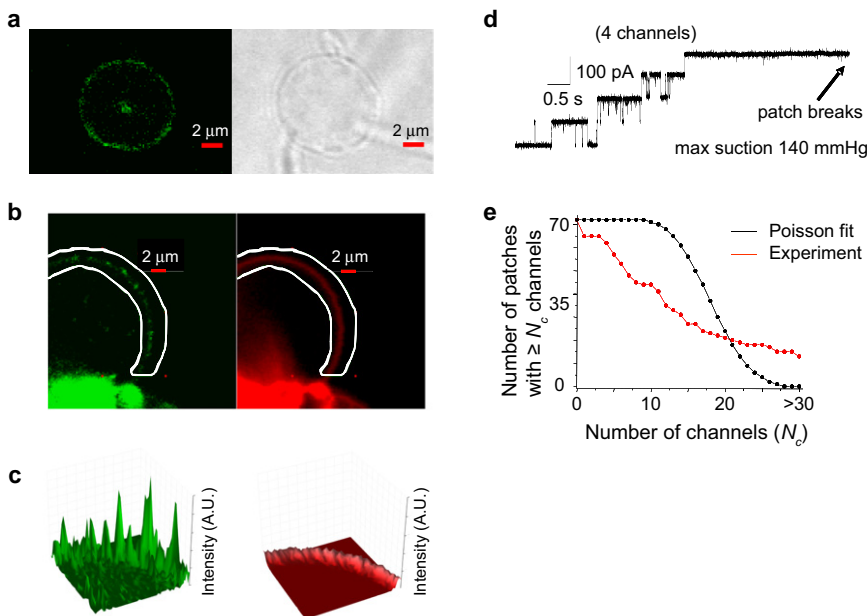


FIGURE 1 MscL channels are nonuniformly distributed in membranes. (*a*) Standard light microscopy (*right*) and confocal microscopy (*left*) of fluorescently labeled MscL proteins in a spheroplast, showing a nonuniform distribution of the labels in the membrane. (*b*) Confocal images of an azolectin liposome reconstituted with a 1:1000 (w/w) protein/lipid ratio of fluorescently labeled MscL (*green*) and spiked with 1% rhodamine-labeled DOPE (*red*). Scale bars indicate $2 \mu\text{m}$. (*c*) Histograms of fluorescence intensity (in relative units) generated from the confocal images shown in *b* (*circled areas*). The histograms indicate clearly that the distribution of MscL is not uniform, whereas the rhodamine-labeled DOPE is uniformly distributed. (*d*) The total number of active MscL channels in azolectin patches reconstituted with a protein/lipid ratio of 1:1000 (w/w) does not follow a Poisson distribution. Shown is an example of a single-channel recording from an excised patch containing four active channels at $+30 \text{ mV}$ when increasing suction was applied to the recording pipette. Note that the single-channel conductance of subsequent openings progressively decreases as more channels open compared with the first opening. (*e*) The cumulative distribution of the number of channels does not follow a Poisson distribution, suggesting that the channels cluster (data from $n = 72$ patches).

particular, DOPE seems to play an important role in MscL insertion. Indeed, a DOPC/DOPE mixture of 30%:70%, with a protein/lipid ratio of 1:4000 (w/w) prepared by the sucrose method (21), yielded a mean number of channels very similar to that obtained from preparations made with azolectin. For MscL reconstituted into bilayers of pure DOPC, the mean number of channels per patch was much lower.

Functional interactions between MscL channels

To probe functional interactions between the channels, we analyzed steady-state recordings of >2 min duration that contained multiple concurrent openings. As a representative example, we present results obtained from a single liposome patch, which showed activity of 11 channels in single-channel recordings when maximum suction was applied (Fig. S1 *a*). When less suction was applied, at most five active channels were observed (Fig. S1 *b*). The observed and estimated steady-state gating probabilities are shown in Table S2. The observed distribution of open channels differs significantly from the Poisson distribution (Fig. 1 *e*). When the single-channel gating probability was estimated from a priori knowledge of the patch with 11 channels, the patch with 11 channels behaved more like a patch with five channels, suggesting that the behavior of the channels was not independent. It is always the case that the number of active functional MscL channels that are detectable by the patch clamp at a given pressure will be lower than the number of reconstituted MscL channel proteins that are expected to be active and behave independently at a given protein/lipid ratio. The observation that the channels behave in a dependent manner, rather than independently, is consistent with the model we propose and discuss here. According to the model, MscL channels in a cluster are indistinguishable from each other before the membrane is stretched. Once the membrane is stretched and under tension, the channels within the cluster separate

into separate subclusters of open and closed channels, consistent with our patch-clamp results.

SANS reveals formation of clusters that cannot be diluted

SANS was used to characterize the self-assembly of MscL in the membrane. In particular, neutron scattering allowed us to separately examine the scattering contributions from different constituents of the sample using proton-deuteron contrast variation (22,23). Working with perdeuterated MscL reconstituted in protonated DOPC lipid vesicles, we were able to isolate the scattering of the protein from the background. We performed measurements on samples in a buffer of 13% D_2O that matched the scattering length density of the protonated lipids, to ensure that the observed SANS data would originate predominantly from the deuterated protein. Fig. 2 *a* summarizes the scattering curves and pair distance distribution functions for three different protein/lipid ratios (1:10, 1:20, and 1:30 w/w). The scattering curves do not correspond to the scattering of a single protein, but the large value of the forward scattering $I(0)$ and a rather strong decay at low q indicate scattering of larger objects. From an analysis of the intensity $I(0)$ at $q = 0$ (22), we estimated the molecular mass of the scattering units to be ~ 20 MDa, corresponding to ~ 200 channels. From the distance distribution function (Fig. 2 *a*), scattering particles with sizes on the order of ~ 100 nm are evident, whereas an individual channel in its closed conformation has a diameter of ~ 5.5 nm (17,18). These observations can be readily explained, as each vesicle carries a large number of channels that are expected to give rise to coherent interference of their scattering amplitudes. All protein on one vesicle should thus be regarded as a single scattering object for scattering in the observed q range. Because the size of these objects was found to approximate the size of the vesicles (diameter ~ 120 nm), the channels seem to cover a large fraction of the vesicle surface. The protein may not extend evenly over the entire surface, however, since

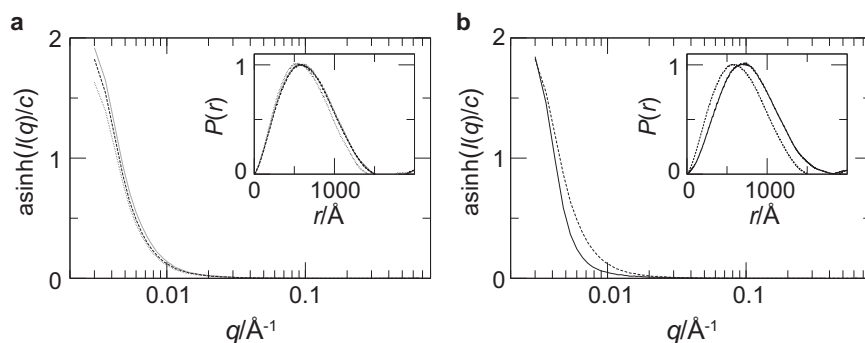


FIGURE 2 SANS intensities indicate clustering of MscL channels that is independent of the protein/lipid ratio. (*a*) SANS of closed MscL channels reconstituted in DOPC vesicles at protein/lipid ratios (w/w) of 1:10 (gray line), 1:20 (dashed line), and 1:30 (dotted line). The intensities are scaled by the channel concentration in μM , which results in equal intensities if the scattering objects scatter incoherently. (*b*) SANS curves of MscL at a protein/lipid ratio of 1:20 (w/w) in the closed (dashed line) and open (solid line) state. The insets show the respective distance distribution functions $P(r)$, obtained by Fourier transformation of the scattering curves. The scaling function $\text{asinh}(x)$ was chosen to display intensities $I(q)$, which is $\sim x$ for small values of x and $\sim \ln(x)$ for large values of x . This way, logarithms of negative numbers for intensities near 0 are avoided.

the scattering curve and distance distribution function do not exhibit the typical features of a hollow sphere (24).

To validate the clustering behavior of MscL in the SANS samples, we analyzed the spatial distribution of the channels across the vesicles. In particular, we considered two limiting scenarios: If the channels do not have a propensity for self-assembly, all vesicles should contain, within statistical variations, the same number of channels (case 1). However, if the channels show a strong tendency for self-assembly, only a fraction of the vesicles should contain protein at some maximum coverage, and the remaining vesicles should be free of protein (case 2).

A first indication of MscL clustering emerges from the number of channels estimated from the forward scattering intensity. From an analysis of the intensity $I(0)$ at $q = 0$ (30), we estimated the molecular masses of the scattering units as 22 MDa, 20 MDa, and 15 MDa, corresponding to 275, 245, and 185 MscL channels, for protein/lipid ratios of 1:10, 1:20, or 1:30 (w/w), respectively. However, if the channels are distributed uniformly over all vesicles, only ~110, 60, or 40 channels per vesicle would be expected, assuming a vesicle radius of ~60 nm as determined by SANS. The estimated number of channels thus exceeds the number expected from a uniform protein distribution by a factor of 3–4, implying a nonuniform distribution of MscL.

Of more importance, the scaling behavior of the forward intensity $I(0)$ when the protein concentration or lipid concentration is varied allows a distinction of the above two protein distribution cases. As is known from scattering theory (24), the forward intensity $I(0)$ depends linearly on the number of scattering particles, and quadratically on the molecular weight of the scattering objects. A distinguishable behavior of the ratio of forward scattering and the protein concentration, $I(0)/c$, follows directly from these dependencies for the different cases of protein distribution (see **Materials and Methods** section for details). In the case of equal protein distribution among all vesicles (case 1), $I(0)/c$ would change with a variation in the protein or lipid concentration. In contrast, in the case of clustering (case 2), $I(0)/c$ would remain constant irrespective of variation in the lipid or protein concentration. We observed the latter behavior in the SANS intensities, as is evident from the superimposed SANS curves in Fig. 2 *a*; hence, the SANS measurements strongly support clustering of MscL. We note that neither the dimensions of the protein scattering objects (see Fig. 2 *a*) nor the size of the vesicles (as determined by SANS at suitable contrast conditions) changed when the channel/lipid ratio was varied, indicating that the observations were not due to changes in vesicle radius.

To verify the presence of functional protein, we added lysophosphatidylcholine (LPC), which was previously shown to open MscL (15,17), to the sample preparations to trap MscL in the open state (Fig. 2 *b*). As expected, we observed an area increase, reflecting the size increase of

the protein cluster as some of the individual channels opened; the maximum of the distance distribution function shifted from ~60 nm to ~75 nm (Fig. 2 *b*, inset). This increase in protein area of ~30–50% after channel opening, observed here for protein clusters (Fig. 2), is smaller than the proposed increase of ~60% expected from the results obtained by EPR spectroscopy and FRET spectroscopy (25), suggesting that not all of the channels are open.

We note that SANS did not reveal any substructure of the cluster; rather, it indicated clustering mainly through the scaling behavior of the signal with varying protein concentration in the sample. To obtain a more direct picture of putative cluster structures, we complemented the SANS results with AFM as an imaging technique.

Demonstration of cluster formation by AFM and neutron reflection studies

Because the fluorescence, patch-clamp, and SANS results all suggested the formation of MscL assemblies, we employed AFM as a complementary visualization technique to further characterize the protein distribution in the membrane. MscL reconstituted in DOPC (at a protein/lipid ratio of 1:10 w/w) was imaged by amplitude modulation (AM) AFM in buffer solution. The AM-AFM images depicted membrane patches with dimensions of a few micrometers (Fig. 3 *a*). Line-like patterns that protruded ~0.5 nm from the 4.7-nm-thick DOPC membrane were visible. These patterns had widths on the order of ~10 nm separated by ~10-nm-wide lines of the flat DOPC bilayer (Fig. 3 *b*). Groups of ~5-nm particles could be resolved within these line-like patterns, consistent with the size of individual MscL channels (Fig. 3 *c*) (17,18). The area of the membrane patch was divided approximately equally between the protein-rich phase and the void bilayer. The

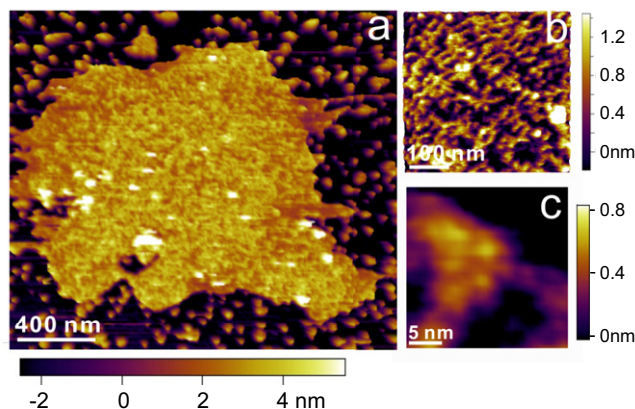


FIGURE 3 AFM reveals spatial clustering of MscL. (a) AM-AFM image of MscL reconstituted in DOPC (1:10 w/w) in phosphate buffer at pH 7.2. The image shows a flat DOPC bilayer with protein assemblies that protrude ~0.5 nm from the membrane. (b) Image showing a magnified area of panel *a*. (c) High-resolution image of the MscL clusters revealing features of ~5 nm that correspond to individual MscL channels.

AFM results thus demonstrate the assembly of MscL into large protein-rich domains, in agreement with the SANS observations, and reveal an additional subpattern that is not resolvable by SANS.

Indications for clustering were also observed in neutron reflectivity experiments with MscL reconstituted into solid-supported DMPC bilayers (Fig. S2, for details see Materials and Methods section in the Supporting Material). By determining the surface coverage from the reflectivity, we identified a layer consisting of ~75% protein and 25% lipids, in contrast to the 7% protein content expected from the composition of the deposited vesicles. The high affinity of the protein for the surface may be a result of protein clustering.

Self-assembly into small clusters via membrane-mediated interactions

Because our AFM images (Fig. 3) indicated a membrane deformation on the order of the hydrophobic mismatch between MscL (hydrophobic thickness ~4 nm) and the bilayer (thickness ~3.5 nm), we sought to determine whether the membrane itself can mediate interactions between channels that will result in spatial clustering and gating statistics that deviate from a Poisson distribution. The energetics of elastic bilayer deformations allow membrane proteins in close proximity to influence equilibrium conformation in both directions, resulting in a tendency to spatially organize on the basis of geometry (26,27). For MscL, we previously demonstrated that such membrane-mediated interactions (shown schematically for two MscL proteins in Fig. 4 *a*) are sufficient to induce cooperative gating (28). The conformational change upon channel opening can severely alter the separation between two proteins, as the tilting of the MscL helices is accompanied by a significant decrease in transmembrane thickness (15,17). The tendency for pairs of MscL channels to cooperatively gate can therefore increase by several orders of magnitude, with a similar reduction in their average separation (28). The interaction potential extends over a length scale of ~4 nm beyond the protein surface, leading to an average center-to-center separation ranging from 5 to 11 nm (28) de-

pending on the protein conformation. This phenomenon is conceptually similar to the hydrophobic effect, in which membrane proteins with similar geometries group together to minimize hydrophobic mismatch. This model is supported by recent electrophysiology and FRET experiments on gramicidin A channels (10), the bacterial potassium channel KcsA (11), ryanodine receptors (8,9), and rhodopsin oligomerization (12).

Self-assembly into clusters is predicted to occur for larger numbers of closed MscL channels as well, since the most energetically favorable state of a membrane that is populated with any number of closed channels corresponds to a single cluster. Moreover, cooperative gating within a cluster can also occur as long as every protein is free to sample both the open and closed states. To illustrate this effect, we developed a computational model that minimizes the membrane free energy G due to bending, area stretch, and tension for an arbitrary arrangement of open and/or closed channels (28, for details see Materials and Methods section in the Supporting Material). Using this model, we quantitatively determined the strength of the elastic interactions between two channels in any combination of states shown in Fig. 4 *a*, and demonstrated that these interactions are sufficient to drive clustering of large numbers of proteins of the same conformation (28).

Proteins within a large cluster may, however, be sterically constrained by their neighbors. To illustrate this point, we considered a cluster of seven MscL proteins with a central protein surrounded by six equidistant neighbors (Fig. 5 *a*). We computed the membrane energy for configurations in which the seven channels remain in a hexagonal arrangement and varied the common distance d between each nearest-neighbor pair (Fig. 4 *b*). For a cluster of all closed channels, the membrane energy is minimized when the center-to-center separation is equal to the channel diameter of 5 nm, which corresponds to the state with minimal hydrophobic mismatch since neighboring channels mask part of the protein-lipid interaction surface. However, cooperative gating from the closed to the open state that is initiated by opening of the central channel cannot occur until the surrounding channels increase their separation by an

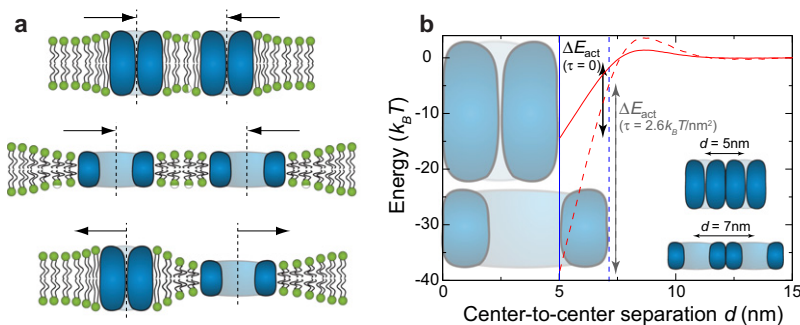


FIGURE 4 Elastic, membrane-mediated interactions generate spatial clustering and cooperative gating of small MscL clusters. (*a*) The hydrophobic mismatch between the lipid bilayer and MscL proteins generates pairwise interactions between two closed channels (*top*), two open channels (*middle*), and one open and one closed channel (*bottom*). The pairwise potentials were determined previously (28). (*b*) Elastic potential for a cluster of seven closed channels arranged in a hexagonal lattice as a function of nearest-neighbor center-to-center separation d . The activation barrier ΔE_{act} for central channel gating is the difference in potential energy between $d = 5$ nm (*solid blue line*, with two closed channels in direct contact) and $d = 7$ nm (*dashed blue line*, with two open channels in contact). The solid red curve is calculated at zero tension ($\Delta E_{act} = 13 k_B T$, shown in black), and the dashed curve is for tension $\tau = 2.6 k_B T / \text{nm}^2$ ($\Delta E_{act} = 32 k_B T$, shown in gray).

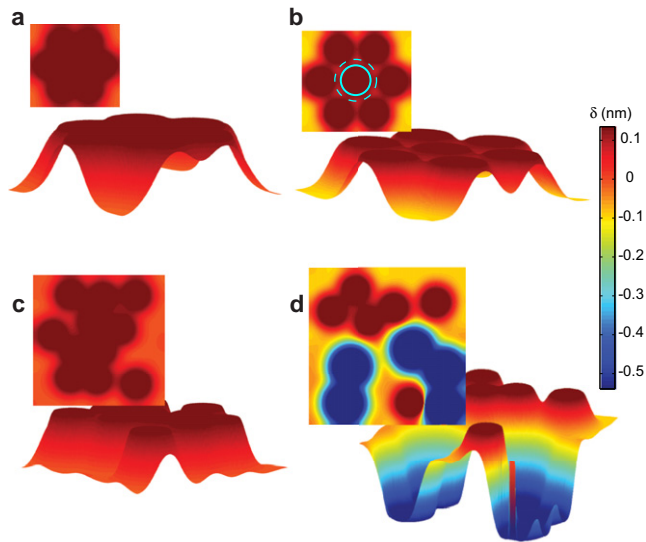


FIGURE 5 Membranes with a high density of MscL channels can exhibit a wide range of clustering behaviors. (a) Top and side views of the membrane profile of a cluster of seven closed MscL proteins in a close-packed hexagonal array with a minimal channel separation of $2r_{\text{closed}} = 5$ nm. The shading indicates the membrane deformation δ relative to the relaxed leaflet thickness, indicated by the color bar in nanometers. (b) A membrane profile with increased separation (7 nm, *dashed cyan circle*) has greater hydrophobic mismatch and hence higher elastic energy than the minimal 5-nm separation (*solid cyan circle*), but allows for unhindered gating of the central channel. (c) Crowded patch of membrane containing 11 proteins in the closed state, illustrating minimal hydrophobic mismatch between channels. (d) A membrane patch under high tension, with five of the 11 proteins gated into the open state, segregates into smaller clusters due to steric constraints on protein gating.

additional 2 nm (see *dashed and solid circles* representing the open and closed channel diameters, respectively, in Fig. 5 b).

To evaluate the consequences of this steric constraint, we computed the change in membrane energy for such a cluster of seven channels in a hexagonal arrangement for different center-to-center channel separations (Fig. 4 b). At zero tension, the membrane energy at their minimum separation of 5 nm is reduced by $\sim 14 k_B T$ relative to configurations in which the channels are too far apart to interact (*solid red curve*), whereas the reduction in membrane energy for open channels at their minimum separation of 7 nm is much larger. However, the reduction in membrane energy for a cluster of closed channels at a 7-nm separation is only $\sim 1 k_B T$. Therefore, achieving this separation requires an energy input of $\Delta E_{\text{act}} = 13 k_B T$ (*black double-headed arrow* in Fig. 4 b), an activation barrier that can slow the cooperative gating of a large cluster in a crowded membrane by several orders of magnitude. The magnitude of this energy barrier will depend on the detailed arrangement of the proteins, and will be larger for clusters with more proteins. Moreover, at higher tensions, the strength of the closed-closed pairwise interaction increases due to the increase in hydrophobic mismatch between the closed channel height and the thinner membrane (28). Similarly,

the interaction energy for the cluster of closed channels also increases to $\sim 38 k_B T$ at the minimum 5-nm separation. Thus, despite the increase in the probability of a single, isolated channel being found in the open state, the activation barrier actually increases in magnitude (for $\tau = 2.6 k_B T/\text{nm}^2$, $\Delta E_{\text{act}} = 32 k_B T$; *gray arrow* in Fig. 4 b). In Fig. 5 c, we show a representative configuration of a membrane surface with 11 closely packed channels in a closed state mimicking the distribution of crowded proteins in the AFM image in Fig. 3 c. In the patch shown in Fig. 5 d, we have assumed that proteins either gate with a probability limited by crowding, or diffuse away to form smaller clusters, producing a partially gated patch, similar to the conclusion drawn from Fig. S1.

DISCUSSION

Functional relevance of MscL clustering

Our observations, as well as previous results from fluorescence studies of labeled MscL in *E. coli* cells, suggest a nonuniform distribution of MscL channels, with a higher density at the poles (Fig. 1 a) (16,29). Although the precise mechanism by which the channels cluster is unclear, cytoskeletal elements and anchoring proteins are not essential for the process, since cluster formation is also visible in azolectin liposomes (Fig. 1 a). Hence, the mechanism of clustering must be related either to the lipid environment or to the intrinsic properties of the MscL protein. The affinity of a protein to a lipid in a microdomain could lead to cluster formation, as was previously demonstrated for cardiolipin-mediated localization of ProP and MscS in *E. coli* (29,30). However, azolectin is not composed of a pure lipid (31), and no obvious rafts were observed in confocal images of the blisters formed by the addition of 1% rhodamine-labeled DOPE. Because clustering was also observed in pure DOPC membranes, it seems unlikely that rafts are the primary mechanism for the formation of these MscL assemblies.

It is well established that in the case of a homogeneous mixture of independent channels, the distribution of the number of channels in a patch should be distributed according to a Poisson distribution. However, we found in our patch-clamp experiments that the distribution of the number of channels deviated significantly from a Poisson distribution (Fig. 1 e). We made this observation after preparing liposomes by different methodologies (dehydration/rehydration and sucrose method) (19,21,32), and using mixtures of DOPC/DOPE or pure DOPC alone. Hence, even if membrane structure plays an essential role in the functioning of MscL and defines some of its biophysical properties (15), the primary mechanism of the cluster formation cannot be attributed only to the properties of a specific component of the bilayer. The primary mechanism may be predicated on some property of the MscL protein itself.

It is conceivable that the methodology used to prepare the liposomes, especially the use of detergent-solubilized MscL (which may also contain some annular lipids), may lead to MscL being inserted as a cluster of proteins. However, because the lateral mobility of proteins within bilayers is well documented (33), and significant diffusion would occur within the time frame of our experiments, the channels should have assumed a uniform distribution in the absence of interactions that cause self-assembly, which is clearly not the case.

Very weak homophilic protein-protein interactions leading to cluster formation have been demonstrated in the case of syntaxins (7), and therefore such a mechanism could also be responsible for the MscL cluster formation observed in this study. Approximately half of the area in the protein-rich patches observed by AFM seems to contain closely packed protein (Fig. 3). Furthermore, the SANS measurements indicate that in a vesicle containing clusters, between 10% and 30% of the area is occupied by protein (Fig. 2), resulting in an upper limit for the interprotein distance of 15 nm, again supporting the notion of high protein density in the clusters. Despite close packing, the channels seem to be embedded in a local environment of lipids, because they remain functional and can be opened, for example, by manipulation of the bilayer environment by the addition of lysolipids.

SANS and AFM revealed the area of the MscL clusters to be rather large, extending up to $\sim 10000 \text{ nm}^2$ and containing clusters with several hundred channels. In patch-clamp experiments, approximately one-third of the patches contained more than 30 active channels per patch. The actual cluster sizes observed likely depend on the experimental technique used and may not be meaningful in the cellular context. However, these large assemblies are a strong indication that attractive protein-protein interactions cause self-assembly. Syntaxin clustering was limited by a balance of attractive protein-protein interactions with sterically unfavorable accommodation of extramembranous filaments in the protein-rich patch (7). Large extramembranous segments are absent in the case of MscL, and the lack of a similar restriction may lead to the observed extended protein domains.

The close packing of the channels raises the possibility that they may be in direct physical contact with each other. Indeed, in steady-state recordings longer than 2 min, in which the number of channels in the patch was known a priori, the probability of observing the different levels of concurrent openings did not follow a Poisson distribution (Table S2 and Fig. 1, *d* and *e*). The poor fit of the kinetic data to a Poisson distribution therefore suggests that the channels were not acting independently. When both the number of channels in the patch and the probability of a single channel being open were estimated assuming independence of channels, the best estimate for the number of channels was always lower than the actual

number of channels in the patch (Table S2 and Fig. S1). These observations suggest that opening a channel somehow decreases the likelihood of other channels opening, indicating that clusters containing 30 active channels observed by patch clamping could contain ~ 100 or more channels, in similarity to the cluster sizes observed by SANS. Further support for this notion comes from the area increase observed by SANS (Fig. 2 *b*) when the channels within a cluster were trapped in an open state by addition of LPC. The increase in protein area of $\sim 30\text{--}50\%$ upon channel opening (Fig. 2) is smaller than the proposed increase of $\sim 60\%$ expected from the results obtained by EPR spectroscopy. Given that the difference between the upper bound of the SANS and EPR experiments is only 10%, which could be within measurement error, this observation suggests that most channels were activated by LPC, and a relatively smaller proportion of channels remained closed in the SANS experiments. Of importance, the LPC experiments thus suggest that even when it is closely packed within the cluster, MscL remains active and mechanosensitive.

How can this observed reduction in channel activity be explained as a consequence of MscL adaptation to the lipid environment? Considering that hydrophobic mismatch is an important determinant of the opening threshold of MscL channels (15), it is not surprising that the likelihood of other channels opening next to an already open channel is increased, simply due to the thinning of the bilayer resulting from the first open channel (28). The origin of cooperative gating lies in the elastic membrane deformations that mediate functional interactions between MscL channels. In large clusters, however, several factors will act in opposition to the tendency for cooperative gating. In Fig. 5 *b*, the stable equilibrium for the ring of surrounding proteins at a separation of 7 nm does not occur with all channels equidistantly spaced; rather, the closed channels are likely to form smaller clusters due to the concavity of the potential favoring local assembly of closely packed small clusters over a global intermediate separation (28). A further effect that counteracts the tendency of proteins to gate cooperatively is the repulsive interaction between an open and a closed channel due to their extreme hydrophobic mismatch over short distances (see *third panel* in Fig. 4 *a*). These factors compete with the tendency of MscL to gate cooperatively, driving the central protein away from the surrounding clusters (which themselves face an energetic barrier to gating similar to ΔE_{act}). The diffusive timescale for MscL across 4 nm ($\sim 10^{-5}\text{--}10^{-4}$ s, assuming a diffusion constant $D \approx 0.1\text{--}1 \mu\text{m}^2/\text{s}$ characteristic of translational diffusion of membrane proteins (33)) is similar to the timescale required for gating. We therefore assume that even under high tension, the gating probability is likely to be reduced by repulsive interactions with neighboring proteins in the open state, in accordance with the experimental findings.

TABLE 1 Cross-technique comparison of the distances between channels in a cluster and cluster sizes

Method	Distance between channels in a cluster	Cluster size
SANS (Fig. 2)	<15 nm	>150 channels (limited by vesicle geometry)
AFM (Fig. 3)	~5 nm	Up to micrometer size
Continuum mechanics model (Figs. 4 and 5)	<6 nm ²⁷	Any size (predicted to be state-, density-, and tension-dependent)

Although the average number of MscL channels is only 3–5 during most of the bacterial life cycle, this number may significantly increase during the stationary phase (1,34), suggesting that MscL clustering plays a role in bacterial physiology. Although the levels of MscL expression during the stationary phase are currently unknown, there is evidence that up to ~50 MscL channels (~10 times the basal level of expression) can be expressed in the bacterial cell membrane (35). Bacterial cells thus appear to be well equipped to protect themselves from the deleterious effects of osmotic forces by the capacity of their cell membranes to accommodate an adequate number of MscL channels when required, as is the case during stationary growth when the cell wall is remodeled and its strength alone is insufficient to protect the cells (1,34). Other mechanosensitive ion channels, such as plant channels, have also been reported to form clusters (36). Thus, cluster formation appears to be a common and functionally important feature of mechanosensitive ion channels. Theoretical considerations of bending energy suggest that polar localization in micron-sized, rod-shaped bacteria based on curvature sensing by single proteins is highly unlikely, but aggregation can enable clusters to preferentially localize to the slightly more curved poles (37,38). In general, protein clustering as a phenomenon presents a new challenge to biophysicists, since the clusters may not only function as protein reservoirs but likely also serve specific functions as molecular machines or stabilizers of protein conformations (13).

CONCLUSIONS

In this study, we combined a variety of experimental and computational techniques to study MscL protein clustering and its functional consequences on channel gating. Although MscL proteins are closely packed within a cluster, they remain active and mechanosensitive. Channel activity, however, is modulated by the presence of the neighboring proteins, indicating membrane-mediated protein-protein interactions. Our implementation of a wide spectrum of experimental conditions did not always result in numerically identical observations; nonetheless, we obtained a very consistent picture of MscL self-assembly leading to clusters with reproducible properties (Table 1). First, all techniques indicated the formation of rather large clusters. Even though the exact cluster size may be limited by the membrane morphology intrinsic to the respective preparation methods (e.g., vesicles in SANS, supported bilayers

in AFM, and blisters in patch-clamp experiments), all of the techniques yielded clusters of tens to hundreds of channels. Second, we obtained comparable measurements of interchannel distances of <15 nm within a cluster, and this result was consistent regardless of the experimental method used. Third, SANS measurements of area differences between clusters of closed and open channels suggested that not all channels in a cluster are open; therefore, segregation into domains of closed and open channels is energetically favorable. This observation is consistent with the theoretical model presented in Fig. 5 *d* and the patch-clamp experiments shown in Fig. 1 *e*. All of the methods employed in this study therefore provide a consistent picture of channels whose activity was reduced by the close proximity of the channels in the cluster. Clustering occurs irrespective of the reconstitution method used, over a wide range of protein/lipid ratios (from 1:10 to 1:8000 w/w), and in bilayers of various lipid compositions. Our findings provide evidence that clustering is an intrinsic property of MscL, and therefore is most likely due to lipid-mediated protein-protein interactions.

SUPPORTING MATERIAL

Materials and methods including analysis details of the SANS experiments, results of neutron reflectivity experiments, details of the continuum elastic theory model, four tables, and two figures are available at [http://www.biophysj.org/biophysj/supplemental/S0006-3495\(11\)00070-1](http://www.biophysj.org/biophysj/supplemental/S0006-3495(11)00070-1).

This study was supported by grants from the Australian Research Council and the National Health and Medical Research Council of Australia to B.M. We gratefully acknowledge support by the D-lab (Grenoble, France), Institut Laue-Langevin (Grenoble, France), and ISIS (Didcot, UK). S.L.G and A.S.U. received support from the DFG-Center for Functional Nanostructures, projects E3.4 and E1.2. V.T.F. and A.W. received support from the Engineering and Physical Sciences Research Council under grants GR/R99393/01 and EP/C015452/1, and from the European Union under contract RII3-CT-2003-505925. K.C.H. received support from a K25 award from the National Institutes of Health (GM075000).

REFERENCES

- Booth, I. R., M. D. Edwards, ..., S. Miller. 2005. The role of bacterial channels in cell physiology. *In* Bacterial Ion Channels and Their Eukaryotic Homologs. A. Kubalski and B. Martinac, editors. ASM Press, Washington, DC. 291–312.
- Cruikshank, C. C., R. F. Minchin, ..., B. Martinac. 1997. Estimation of the pore size of the large-conductance mechanosensitive ion channel of *Escherichia coli*. *Biophys. J.* 73:1925–1931.

3. Corry, B., P. Rigby, ..., B. Martinac. 2005. Conformational changes involved in MscL channel gating measured using FRET spectroscopy. *Biophys. J.* 89:L49–L51.
4. Colledge, M., and S. C. Froehner. 1998. To muster a cluster: anchoring neurotransmitter receptors at synapses. *Proc. Natl. Acad. Sci. USA.* 95:3341–3343.
5. Feng, G., H. Tintrup, ..., J. R. Sanes. 1998. Dual requirement for gephyrin in glycine receptor clustering and molybdoenzyme activity. *Science.* 282:1321–1324.
6. Dalskov, S. M., L. Immerdal, ..., E. M. Danielsen. 2005. Lipid raft localization of GABA A receptor and Na⁺, K⁺-ATPase in discrete microdomain clusters in rat cerebellar granule cells. *Neurochem. Int.* 46:489–499.
7. Sieber, J. J., K. I. Willig, ..., T. Lang. 2007. Anatomy and dynamics of a supramolecular membrane protein cluster. *Science.* 317:1072–1076.
8. Marx, S. O., K. Ondrias, and A. R. Marks. 1998. Coupled gating between individual skeletal muscle Ca²⁺ release channels (ryanodine receptors). *Science.* 281:818–821.
9. Baddeley, D., I. D. Jayasinghe, ..., C. Soeller. 2009. Optical single-channel resolution imaging of the ryanodine receptor distribution in rat cardiac myocytes. *Proc. Natl. Acad. Sci. USA.* 106:22275–22280.
10. Goforth, R. L., A. K. Chi, ..., O. S. Andersen. 2003. Hydrophobic coupling of lipid bilayer energetics to channel function. *J. Gen. Physiol.* 121:477–493.
11. Molina, M. L., F. N. Barrera, ..., J. M. González-Ros. 2006. Clustering and coupled gating modulate the activity in KcsA, a potassium channel model. *J. Biol. Chem.* 281:18837–18848.
12. Botelho, A. V., T. Huber, ..., M. F. Brown. 2006. Curvature and hydrophobic forces drive oligomerization and modulate activity of rhodopsin in membranes. *Biophys. J.* 91:4464–4477.
13. Lang, T., and S. O. Rozzoli. 2010. Membrane protein clusters at nanoscale resolution: more than pretty pictures. *Physiology (Bethesda).* 25:116–124.
14. Yoshimura, K., T. Nomura, and M. Sokabe. 2004. Loss-of-function mutations at the rim of the funnel of mechanosensitive channel MscL. *Biophys. J.* 86:2113–2120.
15. Perozo, E., A. Kloda, ..., B. Martinac. 2002. Physical principles underlying the transduction of bilayer deformation forces during mechanosensitive channel gating. *Nat. Struct. Biol.* 9:696–703.
16. Norman, C., Z. W. Liu, ..., B. Martinac. 2005. Visualisation of the mechanosensitive channel of large conductance in bacteria using confocal microscopy. *Eur. Biophys. J.* 34:396–402.
17. Perozo, E., D. M. Cortes, ..., B. Martinac. 2002. Open channel structure of MscL and the gating mechanism of mechanosensitive channels. *Nature.* 418:942–948.
18. Chang, G., R. H. Spencer, ..., D. C. Rees. 1998. Structure of the MscL homolog from *Mycobacterium tuberculosis*: a gated mechanosensitive ion channel. *Science.* 282:2220–2226.
19. Delcour, A. H., B. Martinac, ..., C. Kung. 1989. Modified reconstitution method used in patch-clamp studies of *Escherichia coli* ion channels. *Biophys. J.* 56:631–636.
20. Shapovalov, G., and H. A. Lester. 2004. Gating transitions in bacterial ion channels measured at 3 microns resolution. *J. Gen. Physiol.* 124:151–161.
21. Battle, A. R., E. Petrov, ..., B. Martinac. 2009. Rapid and improved reconstitution of bacterial mechanosensitive ion channel proteins MscS and MscL into liposomes using a modified sucrose method. *FEBS Lett.* 583:407–412.
22. Serdyuk, I. N., N. R. Zaccai, ..., G. Zaccai. 2007. Small-angle scattering. In *Methods in Molecular Biophysics*. Cambridge University Press, Cambridge, UK. 794–836.
23. Zaccai, N. R., K. Yunus, ..., R. J. Falconer. 2007. Refolding of a membrane protein in a microfluidics reactor. *Eur. Biophys. J.* 36:581–588.
24. Svergun, D. I., and M. H. J. Koch. 2003. Small-angle scattering studies of biological macromolecules in solution. *Rep. Prog. Phys.* 66:1735–1782.
25. Corry, B., A. C. Hurst, ..., B. Martinac. 2010. An improved open-channel structure of MscL determined from FRET confocal microscopy and simulation. *J. Gen. Physiol.* 136:483–494.
26. Mouritsen, O. G., and M. Bloom. 1993. Models of lipid-protein interactions in membranes. *Annu. Rev. Biophys. Biomol. Struct.* 22:145–171.
27. Jensen, M. O., and O. G. Mouritsen. 2004. Lipids do influence protein function—the hydrophobic matching hypothesis revisited. *Biochim. Biophys. Acta.* 1666:205–226.
28. Ursell, T., K. C. Huang, ..., R. Phillips. 2007. Cooperative gating and spatial organization of membrane proteins through elastic interactions. *PLOS Comput. Biol.* 3:e81.
29. Romantsov, T., A. R. Battle, ..., J. M. Wood. 2010. Protein localization in *Escherichia coli* cells: comparison of the cytoplasmic membrane proteins ProP, LacY, ProW, AqpZ, MscS, and MscL. *J. Bacteriol.* 192:912–924.
30. Romantsov, T., S. Helbig, ..., J. M. Wood. 2007. Cardiolipin promotes polar localization of osmosensory transporter ProP in *Escherichia coli*. *Mol. Microbiol.* 64:1455–1465.
31. Martinac, B., and O. P. Hamill. 2002. Gramicidin A channels switch between stretch activation and stretch inactivation depending on bilayer thickness. *Proc. Natl. Acad. Sci. USA.* 99:4308–4312.
32. Häse, C. C., A. C. Le Dain, and B. Martinac. 1995. Purification and functional reconstitution of the recombinant large mechanosensitive ion channel (MscL) of *Escherichia coli*. *J. Biol. Chem.* 270:18329–18334.
33. Eddidin, M. 1992. Patches, posts and fences: proteins and plasma membrane domains. *Trends Cell Biol.* 2:376–380.
34. Stokes, N. R., H. D. Murray, ..., I. R. Booth. 2003. A role for mechanosensitive channels in survival of stationary phase: regulation of channel expression by RpoS. *Proc. Natl. Acad. Sci. USA.* 100:15959–15964.
35. Häse, C. C., R. F. Minchin, ..., B. Martinac. 1997. Cross-linking studies and membrane localization and assembly of radiolabelled large mechanosensitive ion channel (MscL) of *Escherichia coli*. *Biochem. Biophys. Res. Commun.* 232:777–782.
36. Haswell, E. S. 2007. MscS-like proteins in plants. In *Mechanosensitive Ion Channels*, Part A. O. P. Hamill, editor. Academic Press, Amsterdam. 329–359.
37. Mukhopadhyay, R., K. C. Huang, and N. S. Wingreen. 2008. Lipid localization in bacterial cells through curvature-mediated microphase separation. *Biophys. J.* 95:1034–1049.
38. Huang, K. C., and K. S. Ramamurthi. 2010. Macromolecules that prefer their membranes curvy. *Mol. Microbiol.* 76:822–832.